Shielding Test of a Model for FBR Irradiation Fuel Transport Cask

A. Ohashi[1], K. Ueki[1], I. Iyori[1], S. Uruwashi[2], S. Iwanaga[2] and S. Takahashi[3]

[1] Nuclear Technology Division Ship Research Institute
6-38-1 Shinkawa, Mitaka, Tokyo 181

[2] Fuels and Materials Division O•arai Engineering Center
Power Reactor and Nuclear Fuel Development Corporation
4002 Naritacho, O•arai-machi, Ibaraki-ken 311-13

[3] Atomic Transport Service Ltd.
3-5-8 Nishi shinbashi, Minato-ku, Tokyo 105

INTRODUCTION

A prototype FBR (Fast Breeder Reactor), MONJU, has been constructed by Power Reactor and Nuclear Fuel Development Corporation in Tsuruga, Japan. The Corporation is going to perform the post-irradiation-experiment of the FBR fuel assembly after the criticality. To do this experiment, the fuels have to be transported by a shipping vessel from the site to the O•arai Technical Center in Ibaraki prefecture, Japan. In order to take safety examinations of the cask used in the post-irradiation-experiment of the fuels (called PIE cask) by the competent authorities, the corporation made a half scale model of the PIE cask. The tests that were required by the safety transport regulations (tests for shielding, drop, fire, etc.) were performed to derive basic data for safety analysis.

The present work reports a part of the test, neutron and gamma-ray shielding experiments and their analyses. In the experiments, the locations of a source and a detector were changed to obtain the dose distribution around the half scale model. And the same states as in the experiments were analyzed by the use of Monte Carlo codes.

For the real scale spent-fuel shipping cask of a light water reactor (LWR), UEKI et al. 1983, have performed shielding experiments and their analyses. The difference between the PIE cask and the LWR's cask exists in shielding ability due to the higher neutron fluence of the FBR fuel assembly. Moreover the PIE cask has uncommon form for the weight limit.

EXPERIMENT

An illustration of the half scale model of the PIE cask is shown in Fig. 1. The length of the half scale model is about 300 centimeters and radial dimension around the body is about 40 centimeters. The main material structuring the model is stainless steel (SUS304). The material shielding gamma ray is lead and neutron is shielded by the antifreezing solution with ethylene glycol. Stainless steel fins of a thin annular structure are attached to the outer surface of the model. Not shown in the figure are bolts, valves, trunnion and other items. The shock absorbers, not included, are usually attached to the lid and the bottom under transport. The PIE cask is characterized by the middle of the body thickening the shielding. As indicated in Fig. 1, the FBR fuel assemblies are entered in the middle of the PIE cask. Moreover the cask is designed for the longer fuel assembly of the pressurized water reactor (PWR).

Shielding experiments were carried out at the Ship Research Institute with a ^{252}Cf neutron source of 4.2×10^{7}

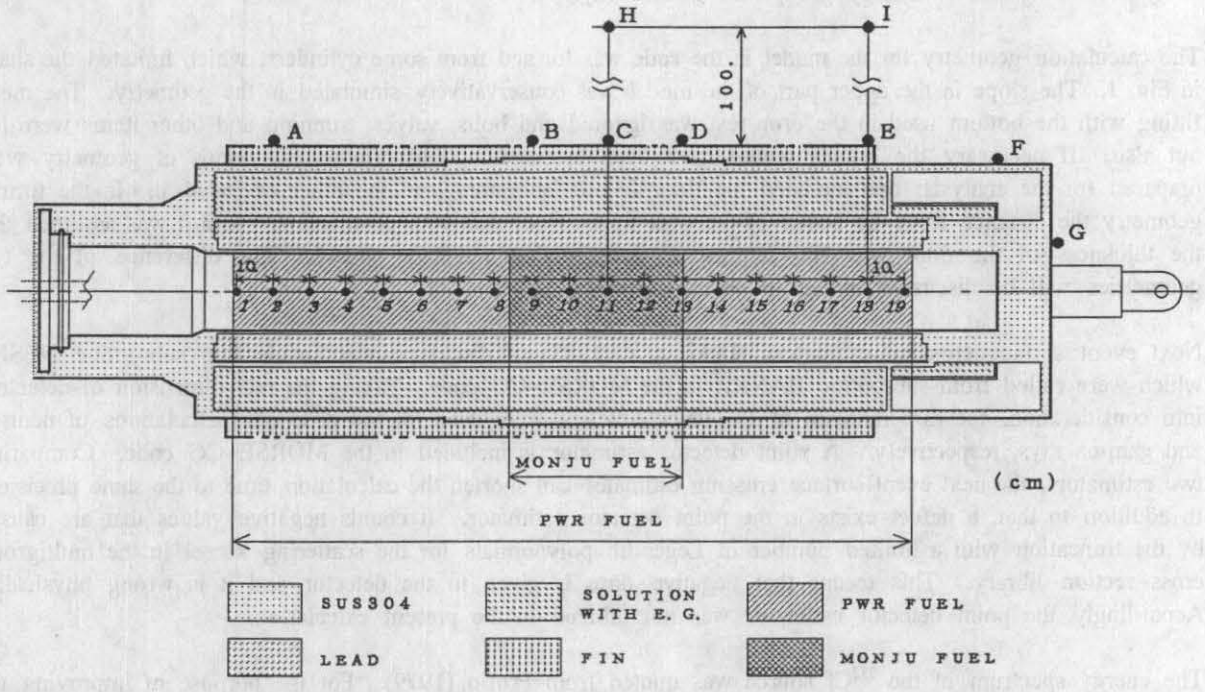

Fig. 1 Illustration of the half scale model of the PIE cask with source locations (1~19) and survey meter positions (A~I).

neutrons per second and a ^{60}Co gamma-ray source of 1.7×10^{8} Bq. Each source was put in turn at the source locations from 1 to 19 at an interval of 10 centimeters in Fig. 1. A guide tube that was made of SUS304 was provided in the model and fixed the source. The dose rate distributions for the neutron and the gamma-ray sources were measured at the detector positions from A to I in the same figure. The detector positions from A to G are located at the surface of the half scale model and the positions from H to I are situated at 100 centimeters from the cask surface corresponding to the safety transport regulations.

A moderation-type survey meter made by ALOKA CO. LTD. (model TPS-451) was used for the measurements of neutron dose rates. The gamma-ray dose rates were measured with an ionization-type survey meter made by the same company (model ICS-315). The variation of the detection efficiency with direction must be paid attention in particular for the measurement of neutron dose rates. Although the detection efficiency changed about 10 percentage points corresponding to the direction of the detector, the direction that normalized detection efficiency was in the direction of the source in the model. No correction of the measured values was carried out. The background of the detector for neutron was ignored as it was small. For gamma rays the background was 5.0×10^{-5} mSv/h affecting largely the measurements of the ^{60}Co gamma ray dose rates.

CALCULATION

A Monte Carlo code, MORSE-CG (Emmett 1975), was used for solving neutron and gamma ray transport problems. A neutron-gamma ray coupled group cross-section library, NGCP9-70 (Ueki et al. 1985), was utilized for the dose rate calculations of neutron and secondary gamma ray. Another group cross-section library, CASK-LIB-50 (Ueki et al. 1983), was employed for the calculation of ^{60}Co gamma ray. These libraries were made from ENDF-B/IV (Garber 1975). The former is constructed by P_9 (maximum Legendre expansion coefficient) and 50 energy groups for neutron and 20 energy groups for gamma ray. The latter is

composed of P_5 and 18 energy groups for gamma ray.

The calculation geometry for the model in the code was formed from some cylinders, which imitated the shape in Fig. 1. The slope in the upper part of the model was conservatively simulated in the geometry. The metal fitting with the bottom used in the drop test was ignored and bolts, valves, trunnion and other items were left out also. If necessary the effects would have been evaluated. Furthermore two kinds of geometry were prepared for the analysis: one included the floor in our laboratory and the other excluded it. In the former geometry the distance from the center of the cask to the floor was 90.5 centimeters. And it was assumed that the thickness of the floor was 100 centimeters and 2000 centimeters square. The difference of the two geometries will be discussed in the following section.

Next event surface crossing estimators (Ueki et al. 1983) of disc type were made into subroutine NESXE which were called from subroutine BANKR in the MORSE-CG code. Taking the real dimension of detectors into consideration, the disc radiuses of 15, 10 centimeters were used for the dose rate calculations of neutron and gamma rays, respectively. A point detector estimator is included in the MORSE-CG code. Comparing two estimators, the next event surface crossing estimator can shorten the calculation time to the same precision. In addition to that, a defect exists in the point detector estimator. It counts negative values that are caused by the truncation with a limited number of Legendre polynomials for the scattering kernel in the multigroup cross-section library. This means that negative dose is given to the detector and it is wrong physically. Accordingly the point detector estimator was not utilized in the present calculation.

The energy spectrum of the ^{252}Cf source was quoted from Profio (1979). For the purpose of improving the precision of calculated values and shortening the calculation time, the relative importance was employed to the source spectrum. It was applied to the energy bins between 13.5 MeV and 275 eV so as not to change very much the weight of the source particles in the MORSE-CG code. For the same reasons, splitting, Russian Roulette and exponential transform were adopted in the calculation. The splitting values were experientially set up, while they were approximately the same values as the attenuation rate. In addition, the number of the scattering particles had to be considered so as to become the same values approximately at the each region of the calculation geometry in each energy bin of the multigroup cross-section library. And the Russian Roulette values were one-tenth of the splitting values. In regard to the exponential transform, the function DIREC in the MORSE-CG code was changed in order to stretch the path length of the particle generated in the code to the radial direction for detector positions A ~ F, H, I and to the axis direction of the model for the detector position G. The dose rates of the detector position G were calculated separately from the others.

A HEWLETT-PACKARD 9000/835 computer was employed in the calculation. In order to calculate one of the calculated values in Figures 2, 3, 4, it took about 0.5 hours for 2000 × 200 histories (the number of particles per batch × the number of batches) by the use of the computer machine. Fractional standard deviations of the calculated values in Figures 2, 3, 4 became 0.024 ~ 0.27, 0.039 ~ 0.22, 0.087 ~ 0.18, respectively. The precision of the values was good but grew worse at long distances from a source location to a detector position.

A continuous energy Monte Carlo code with pointwise cross sections (MCNP, 1981), was used for the calculation of the neutron dose rate in the direction of radius. This code is free from approximations included in the multigroup cross sections and the truncation with a limited number of Legendre polynomials for the scattering kernel. An explanation of the method of this calculation by the use of the MCNP code is omitted from this proceeding and described at another opportunity.

RESULTS AND DISCUSSION

The dose rates of neutron, secondary gamma ray and ^{60}Co gamma ray at source locations 1 ~ 19 are shown in Fig. 2, 3, 4, respectively at the detector position C in Fig. 1. The horizontal axes indicate the source locations. The left figure shows dose rates and the right reveals the ratios of calculation to experiment (C/E).

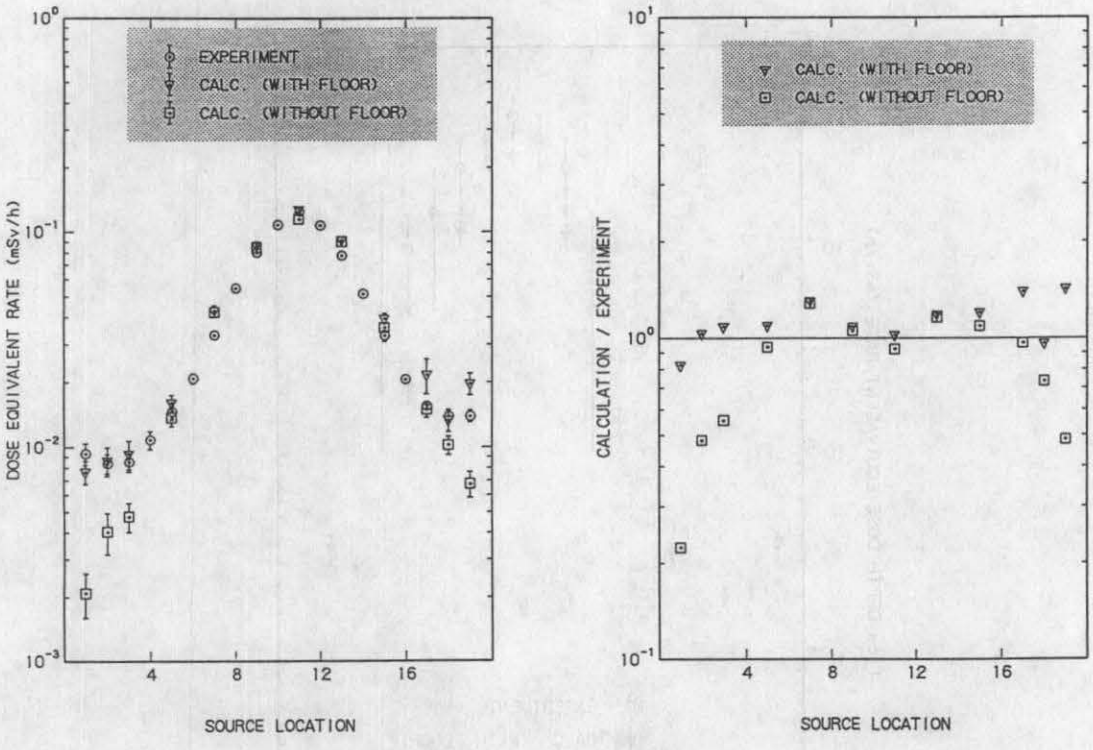

Fig. 2 Comparison of neutron dose rates between measured and calculated values for the detector position C.

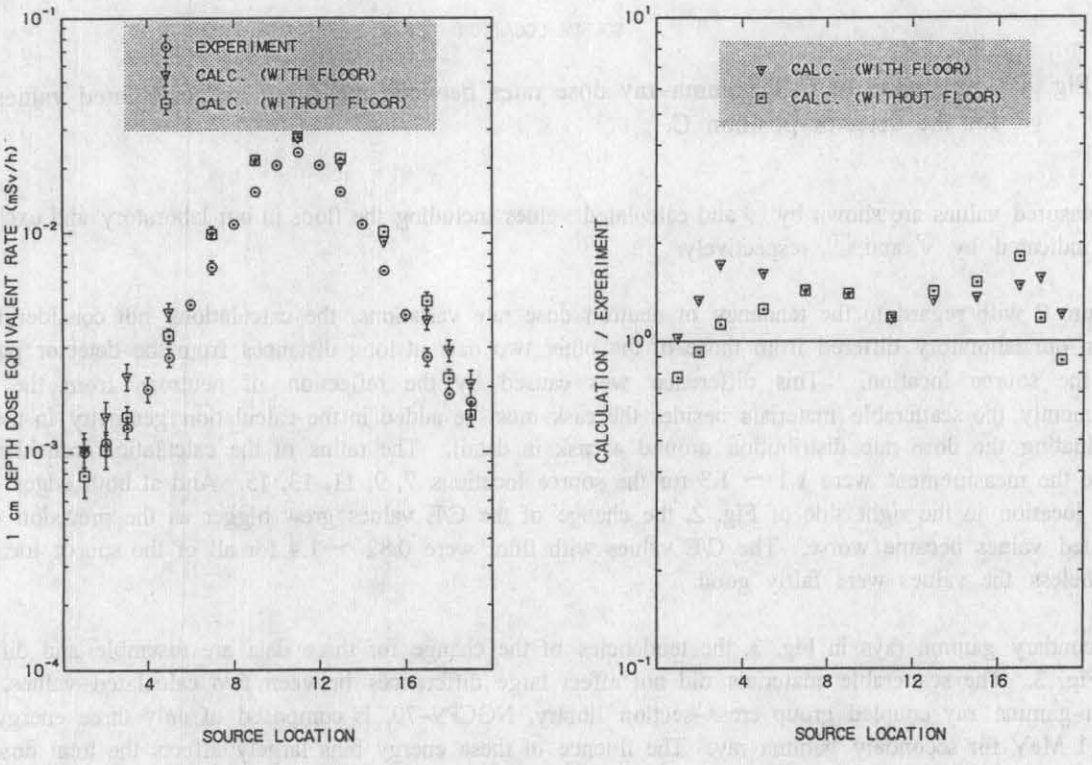

Fig. 3 Comparison of secondary gamma-ray dose rates between measured and calculated values for the detector position C.

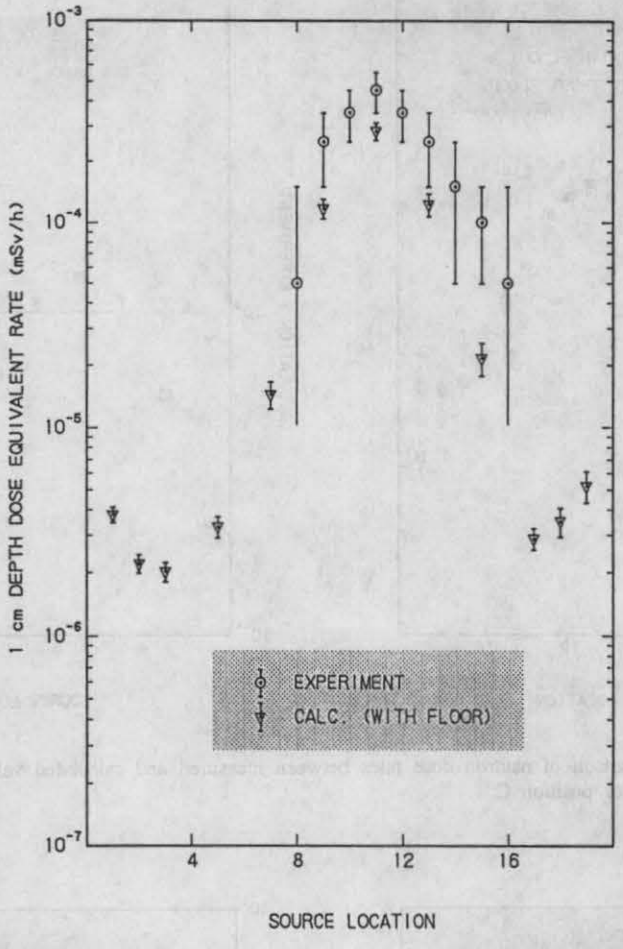

Fig. 4 Comparison of ^{60}Co gamma-ray dose rates between measured and calculated values for the detector position C.

The measured values are shown by ○ and calculated values including the floor in our laboratory and excluding it are indicated by ▽ and □, respectively.

In Figure 2 with regard to the tendency of neutron dose rate variations, the calculations not considering the floor in our laboratory differed from those of the other two data at long distances from the detector position C to the source location. This difference was caused by the reflection of neutrons from the floor. Consequently the scatterable materials besides the cask must be added in the calculation geometry in the case of evaluating the dose rate distribution around a cask in detail. The ratios of the calculation considered in floor to the measurement were 1.1 ~ 1.3 for the source locations 7, 9, 11, 13, 15. And at both edges of the source location in the right side of Fig. 2, the change of the C/E values grew bigger as the precision of the calculated values became worse. The C/E values with floor were 0.82 ~ 1.4 for all of the source locations. Nevertheless the values were fairly good.

For secondary gamma rays in Fig. 3, the tendencies of the change for three data are resemble and different from Fig. 2. The scatterable materials did not effect large differences between two calculated values. The neutron-gamma ray coupled group cross-section library, NGCP9-70, is composed of only three energy bins below 1 MeV for secondary gamma ray. The fluence of these energy bins largely affects the total dose rate of secondary gamma ray. Consequently the errors for the multigroup cross sections are included in this

calculation. The C/E values with floor were 1.0 ~ 1.7 for all of the source locations. For five data in the middle of the source locations, the C/E values were 1.2 ~ 1.5. Though the calculated values overestimate the measured values a little, the values were good.

The neutron source, ^{252}Cf, generated primary gamma rays. The dose rates around the model were calculated by the use of the spectrum of Profio (1979). The contribution of their values to those of secondary gamma ray was about 1 percent and within the secondary gamma-ray calculation error. Though the primary gamma ray is almost shielded by lead inside the PIE cask, secondary gamma rays exist strongly. The magnitude of the dose rates of secondary gamma rays is approximately one-fifth of those of neutrons from Figures 2, 3. In evaluating the shielding effect of the real scale PIE cask, the dose rate of secondary gamma rays must be given attention.

At the detector positions F, G, the calculated values overestimated the measured values for neutron, and for secondary gamma ray the calculation underestimated the measurement. They were affected by the solution in the thermal expansion room since the solution in the room was ignored and treated as the void in these calculation geometries. The solution is good shielding material for neutrons and it generates the secondary gamma rays conversely. For the accurate evaluation of the dose rate in these positions, the solution in the room must be added in the calculation geometry.

For ^{60}Co gamma rays the dose rates are shown in Fig. 4. The calculated values underestimated the measured values. Although the measured values include large errors for the insufficient strength of the ^{60}Co source, the values agree roughly with the calculated values.

Calculated energy spectra for neutron and secondary gamma rays are shown in Fig. 5 at the detector position C for the source location 11. In this figure, a lethargy was defined as the natural logarithm of the ratio of the upper limit to the lower limit of the energy bin of the NGCP9-70 library. A peak of 24 keV for neutrons reveals an iron window. For secondary gamma rays two peaks must be paid attention at 2.2 MeV and 7.6 MeV due to the (n, γ) reaction of hydrogen and iron, respectively. In figure 6, the calculations by the MCNP code show neutron dose rate distribution in the radial direction of the model from the source location 11. The attenuation due to the solution with ethylene glycol is observed clearly. In this region the neutron dose rate became one-fiftieth. The calculated values of the MCNP code agreed closely with the measured valued at the detector position C, H.

CONCLUSION

Shielding experiments and their Monte Carlo analyses of the half scale model of the PIE cask were carried out to

1. obtain the dose rate distributions around the model and deduce the characteristics of the actual cask dose distribution from the results,
2. examine the propriety of calculational techniques and the accuracy of Monte Carlo codes to be used in the shielding design or the analysis of the actual cask.

The following remarks were obtained through the present study.

1. The C/E values were good for almost all the detector locations except for a few particular points.
2. The calculation geometry with scatterable materials around the cask is necessary to derive the details of dose distribution.
3. The solution in the thermal expansion room must be taken into account and added in the calculation geometry.
4. The magnitude of the dose rates of secondary gamma rays is approximately one-fifth of those of the neutron of the half model. Two peaks must be paid attention at 2.2 MeV and 7.6 MeV due to the (n, γ) reaction of hydrogen and iron, respectively.

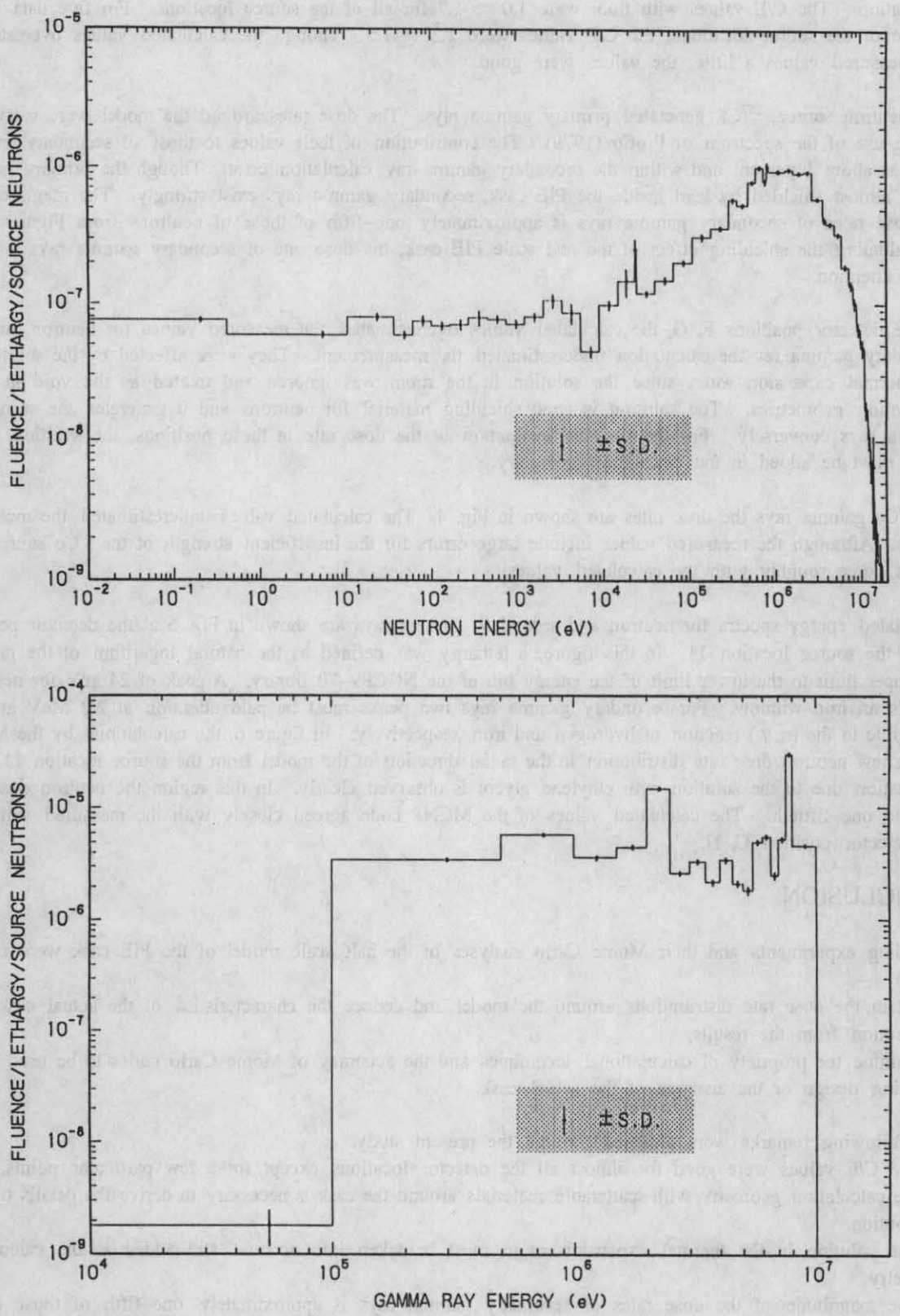

Fig. 5 Calculated energy spectra of neutron and secondary gamma ray for the detector position C at the source location 11. (S. D. : Standard Deviation)

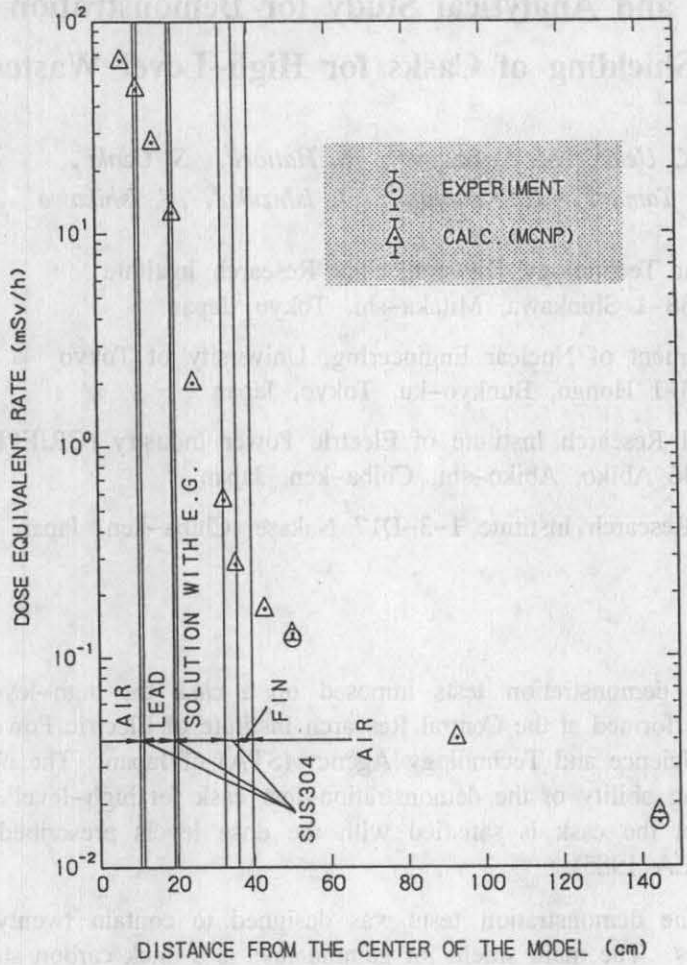

Fig. 6 Neutron dose rate distribution in the radial direction of the half scale model at the source location 11 including two measured values of the detector position C, H.

Hence the calculational techniques that were employed in these analyses can be applied to the design or to the safety analysis of the actual cask, which included the computer codes and the nuclear data. In future for the full scale model of the PIE cask, its shielding effect will be calculated by means of the replacement of the source spectrum from ^{252}Cf to a FBR fuel assembly of post-irradiation-experiment.

REFERENCES

Emmett M. B. The MORSE Monte Carlo Radiation Transport Code System, ORNL-4972, Oak Ridge National Laboratory (1975).

Garber D. (Ed.). ENDF/B summary documentation, BNL-NCS-17541 (ENDF-201), 2nd. ed. (ENDF/BIV), available from the National Nuclear Data Center, BNL (1975).

MCNP-A General Monte Carlo Code for Neutron and Photon Transport, LA-7396-M (Rev.) Version 2, Los Alamos National Laboratory (1981).

Profio A. E. Radiation Shielding and Dosimetry, JOHN WILEY & SONS, New York (1979).

Ueki K., Inoue M. and Maki Y. Validity of the Monte Carlo Method for Shielding Analysis of a Spent-Fuel Shipping Cask : Comparison with Experiment, Nucl. Sci. Eng., 84, 271 (1983).

Ueki K., Ogawa Y., Naito H. and Hyodo T. Analysis of a 14-MeV Neutron Streaming Through a Narrow Hole Duct Using the Monte Carlo Coupling Technique, Fusion Technol., 7, 90 (1985).